CHAPTER IV

RESULTS AND DISCUSSION

A. Characterization of xyloglucan spray dried powder from Tamarind seeds

1. The percentage yield of xyloglucan spray dried powder

The percentage yield, percentage moisture content and physical appearances of the xyloglucan spray dried powders prepared by four different methods are displayed in Table 5. Figure 15 shows the physical appearances of xyloglucan dried powder from four different methods. From all methods, the physical appearances of xyloglucan spray dried powder were whitish powder, mild aggregation and very bulky. The spray dried powder of method I and II were more bulky than those spray dried powder of method III and IV. The %total yield and %moisture content of xyloglucan spray dried powder (from both collecting chamber and cyclone) from four different methods varied from 18.40-26.21 and 6.26-10.81, respectively. It was notable that the percentages moisture content of the powder in cyclone were slightly higher than in collector. The reason might be due to the higher temperature in the cyclone than in collector.

Table 5 Comparison of the percentage yield, percentage moisture content and physical appearances xyloglucan spray dried powder from four different methods

Method	% Total yield	%moisture content		Appearance
		collecting chamber	cyclone	
I	26.21	9.29	6.63	Whitish powder, bulky
II	23.20	10.81	8.93	Whitish powder, bulky
III	18.40	7.27	6.26	Whitish powder, bulky
IV	19.62	9.36	6.36	Whitish powder, bulky

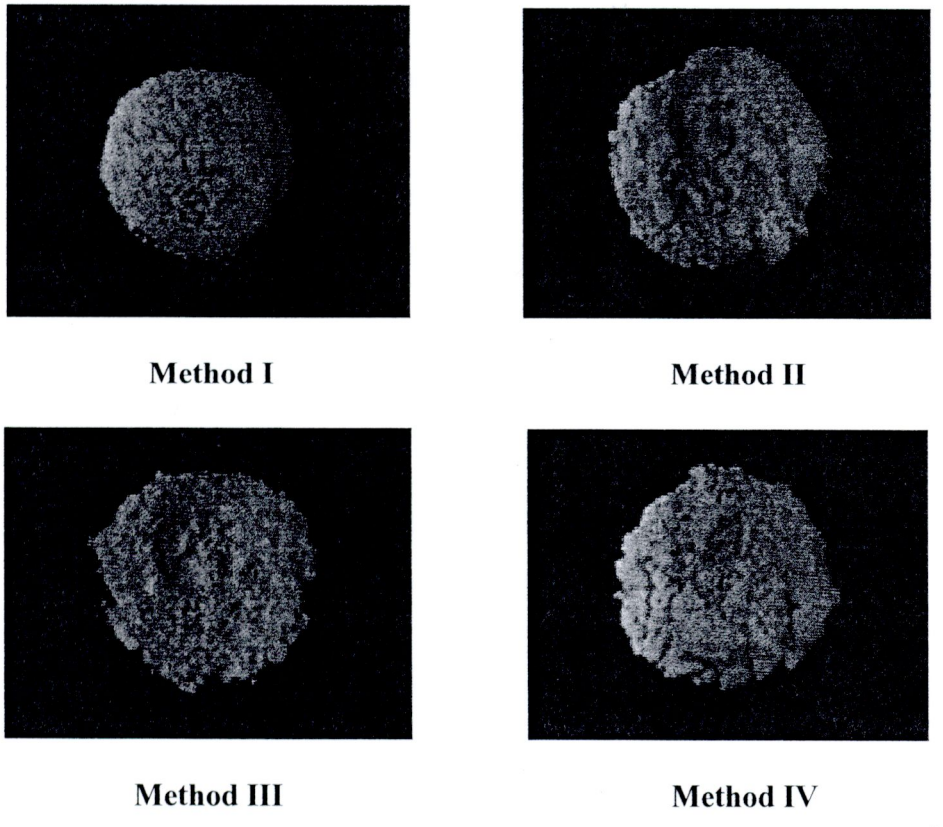

Method I **Method II**

Method III **Method IV**

Figure 15 The xyloglucan spray dried powder from four different methods

2. Determination of xyloglucan in tamarind seed powder

2.1. Validation of HPLC method

The validation of analytical method is the process by which it is established that the performance characteristics of the method meet the requirements for the intended analytical applications. The performance characteristics are expressed in term of analytical parameters. For HPLC assay validation, these include specificity, linearity, accuracy and precision of the method will be determined.

2.1.1 Specificity

The specificity of an analytical method is the ability to measure the analyses accurately and with specificity in the presence of other components in the sample. Figure 16 shows typical chromatograms of standard xyloglucan solution, sample solution and absolute ethanol, respectively. The chromatograms demonstrated that the HPLC condition used in the study had a suitable specificity.

2.1.2 Linearity

The calibration curve data of standard xyloglucan are shown in Table 6. The plot of standard xyloglucan concentrations versus the peak area (Figure 2A) displayed the lnear correlation in the concentration range studied of 400-900 μg/ml. The coefficient of determination (R^2) of this line was 0.9997. These results indicated that HPLC method was acceptable for quantitative analysis of xyloglucan in the range studied

2.1.3 Accuracy

The accuracy of an analytical method is the closeness of test results obtained by the method to the true value. Accuracy is calculated as percent recovery by the assay of known added amount of analyses. The percentages analytical recovery of xyloglucan was in the range of 98.14-100.68% which indicated that this method could be used for analysis in all concentrations studied with a high accuracy (Table 7).

2.1.4 Precision

The precision of xyloglucan analyzed by HPLC method were determined both within run precision and between run precision as illustrated in Tables 3A and 4A. All coefficients of variation values were small, as 0.43-1.04% and 1.15-1.78%, respectively. The coefficient of variation of an analytical method should generally be less than 2%. Therefore, the HPLC method was precise for quantitative analysis of xyloglucan in the range studied.

3. The percent xyloglucan, total protein and fat of xyloglucan spray dried powders

The percentage contents of xyloglucan, total protein and fat of xyloglucan spray dried powder from four different methods and tamarind seed powder are shown in Table 10. The results were obtained by the analysis of variance (ANOVA) at significant level 0.05. According to analytical statistics, all of the methods could significantly reduce the contaminated fat. Moreover, Method I, II and III also reduced significantly the contaminated of protein. However, it revealed that methods resulted to no significant difference of the %xyloglucan content.

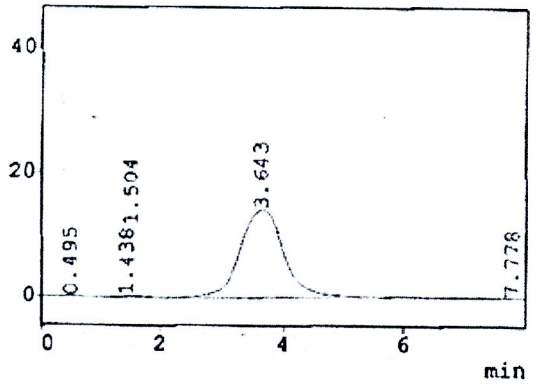

(a)

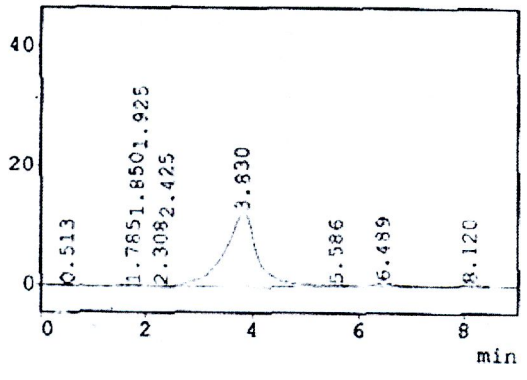

(b)

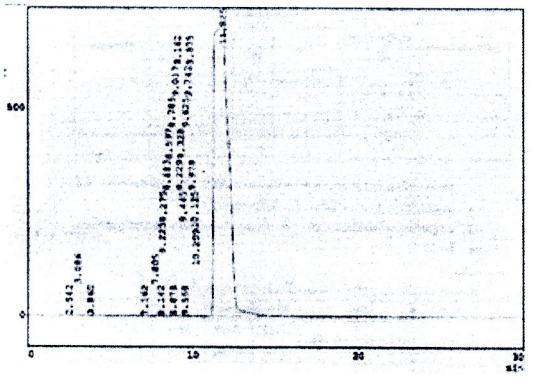

(c)

Fig 16 HPLC chromatograms of ultrapure water

(a) xyloglucan standard solution

(b) sample solution

(c) absolute ethanol

Table 6 Data of calibration curve of xyloglucan by HPLC method

Concentration (µg/ml)	Peak area			Mean	SD	%CV
	Set1	Set2	Set3			
400	3140440	3136673	3127925	3135012.67	6420.58	0.20
500	3946311	3942877	3962926	3950704.67	10722.35	0.27
600	4766031	4718676	4729805	4738170.67	24761.10	0.52
700	5503701	5384933	5497697	5462110.33	66904.91	1.22
800	6309434	6156137	6268376	6244649.00	79355.03	1.27
900	7172318	6924533	7072993	7056614.67	124701.80	1.77
R^2	**0.9996**	**0.9994**	**0.9998**	**0.9997**	-	-

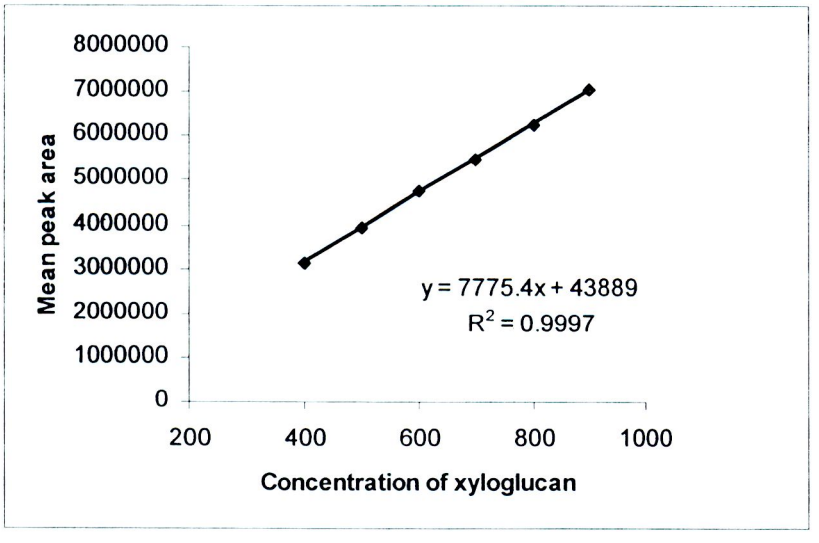

Fig 17 Calibration curve of xyloglucan by HPLC method

Table 7 The percentages of analytical recovery of xyloglucan by HPLC method

Concentration (µg/ml)	%Analytical recovery					Mean ± SD
	1	2	3	4	5	
450	98.35	100.16	99.19	98.12	100.40	99.24 ± 1.03
650	100.68	100.40	100.31	100.46	98.66	100.10 ± 0.82
850	98.77	99.14	98.62	98.16	98.14	98.56 ± 0.43

Table 8 Data of within run precision by HPLC method

Concentration (µg/ml)	Concentration (µg/ml)					Mean	SD	%CV
	Set1	Set2	Set3	Set4	Set5			
450	442.56	450.71	446.33	441.52	451.78	446.58	4.64	1.04
650	654.42	652.59	652.02	652.97	641.30	650.66	5.31	0.82
850	839.55	842.68	838.23	834.32	834.16	837.79	3.62	0.43

Table 9 Data of between run precision by HPLC method

Concentration (µg/ml)	Concentration (µg/ml)					Mean	SD	%CV
	Set1	Set2	Set3	Set4	Set5			
450	446.58	465.2	458.43	446.26	452.87	453.87	8.08	1.78
650	650.66	670.94	648.16	644.65	653.07	653.50	10.24	1.57
850	837.79	862.6	842.4	854.29	850.74	849.56	9.79	1.15

Molinarolo (1990) and Sumathi and Ray (2002), a large amount of ethanol was used in extraction of xyloglucan, resulting to high cost of production. In this research, the step of precipitation of xyloglucan with ethanol was removed. Moreover, the defatting with hexane was added in the process of xyloglucan extraction, consequently, xyloglucan powder had low contamination of fat.

Table 10 Comparison of the percentage contents of xyloglucan, total protein and fat of xyloglucan spray dried powder from four different methods and tamarind seed powder (mean ± SD)

	% xyloglucan	%Protein	%Fat
Tamarind seed powder	-	15.87 ± 0.35	7.73 ± 0.27
Method I	42.85 ± 0.92	14.35 ± 0.12*	1.09 ± 0.17*
Method II	43.72 ± 0.49	14.17 ± 0.08*	1.15 ± 0.16*
Method III	42.90 ± 1.11	14.64 ± 0.33*	0.89 ± 0.34*
Method IV	44.62 ± 0.92	15.19 ± 0.29	1.19 ± 0.17*

* Significant at *P value* = 0.05

4. Morphology of xyloglucan spray dried powder

Figure 18 represented the scanning electron microscopy (SEM) of xyloglucan spray dried powder of four different methods. Particles of all methods were very small and spherical shaped, but some were shrunk and aggregated. The surface particles of xyloglucan spray dried powder from method I and II were rather smooth but method III and IV were rough with shrunk surface.

The results could be explained that method of xyloglucan extraction had effect on the surface topography of particles. In method III and IV, the defatting process by hexane was done with slurry of tamarind seed powder in water.

As the results, all four methods could reduce the %contaminated of total protein and fat. However, defatting process of method III and IV had effect on morphology of xyloglucan spray dried powder. Thus, method III and IV were not suitable for the xyloglucan extraction from tamarind seed. The method II was more time-consuming than method I since it had to leave standing overnight. Consequently, method I was the most appropriate method for xyloglucan extraction

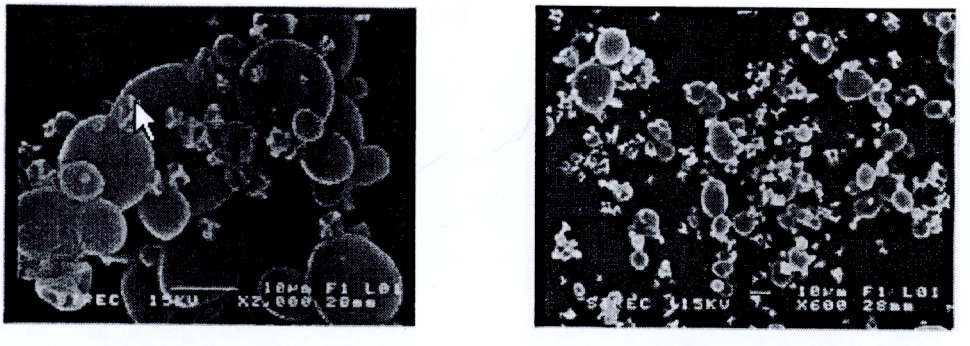

(× 2000) (×600)

(a)

Figure 18 Scanning electron photomicrographs of xyloglucan spray dried powder from four different methods; (a) Method I, (b) Method II, (c) Method III and (d) Method IV

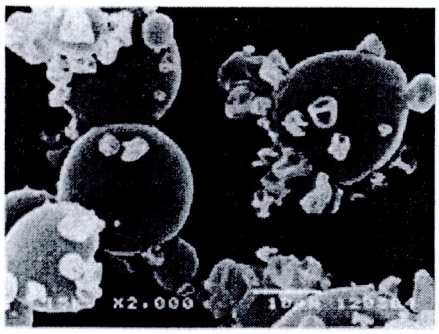

(× 2000)

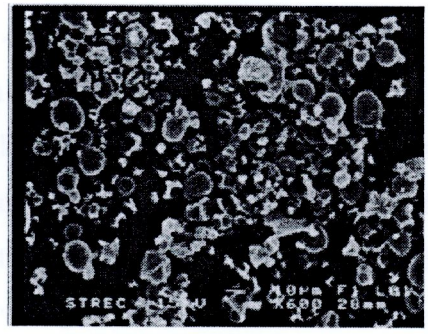

(×600)

(b)

(× 2000)

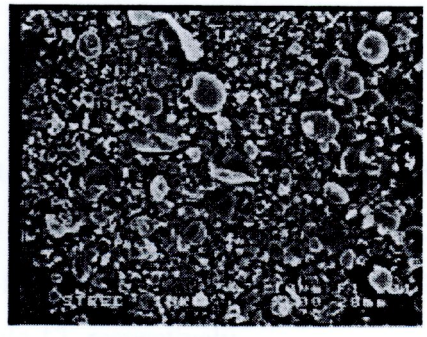

(×600)

(c)

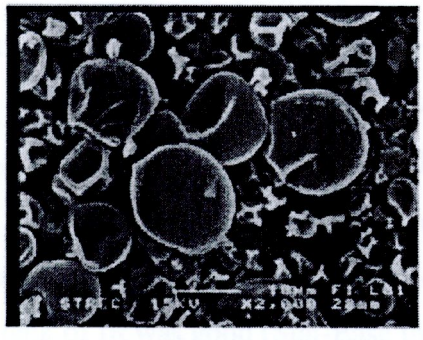

(× 2000)

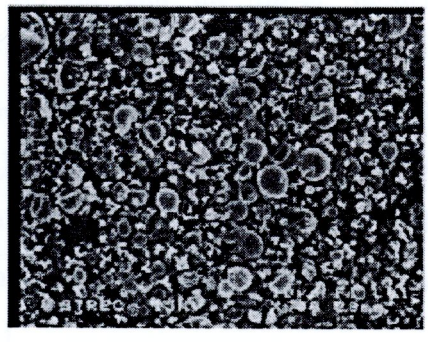

(×600)

(d)

Figure 18 Scanning electron photomicrographs of xyloglucan spray dried powder from four different methods; (a) Method I, (b) Method II, (c) Method III and (d) Method IV (continued)

B. Optimization of spray drying condition.

1. Optimization of spray drying condition on production yield and moisture

There were many factors effected on yield and powder properties such as concentration of the sample, inlet and outlet air temperature, air flow rate and feed flow rate. In this report, the effect of inlet temperature and air flow rate on the yield and moisture content of spray dried powder were investigated, whereas feed flow rate was fixed at 10%.

To explore the region of the response surface in the neighborhood of the optimum, a second order approximation to the response surface could be developed. A face centered design was used for this purpose. The design matrix with responses is given in Table 11.

The percentage yields and moisture contents varied from 33.64-64.49% and 4.99-7.83%, respectively. The results of the second order, response surface quadratic model fitting in the form of analysis of variance for %yield and the linear model for %moisture content are given in Table 12 and Table 13, respectively.

The analysis of variance of the regression model states that the model of %yield and %moisture content was significant ($P < 0.05$). The response surface quadratic model was an adequate model for %yield and the linear model for %moisture content, as were evident from the F-test ($F_{\%yield} = 10.83$ and $F_{\%moist} = 58.08$) and a very low probability values (%yield: $P_{model} > F = 0.0034$ and %moisture content: $P_{model} > F < 0.0001$) (Table 12 and Table 13). Values of "Prob > F" were less than 0.05 indicated that model terms were significant ($P < 0.05$) (Myers and Montgomery, 2002). Lack of fit for both models was not significant ($P > 0.05$). Non significant lack of fit was good (Stat-Ease Inc., 2005).

The goodness of fit of the models was checked by the determination coefficient (R^2). The value is always between 0 and 1. The closer the value is to 1, the model is stronger and better predict the response (Myers and Montgomery, 2002). In this study, the values of $R^2 = 0.8856$ and 0.9207, indicated that 88.56% and 92.07% of variability in the response could be explained by the model for %yield and %moisture content, respectively (Table 14).

Table 11 A face centered design matrix of two parameters and the observed responses

Code	Factor		Responses	
	Inlet temperature (°C)	**% Aspirator**	**%yield**	**%moisture**
C1	120 (-)	80 (-)	33.64	7.83 ± 0.10
C2	200 (+)	80 (-)	46.80	6.05 ± 0.12
C3	120 (-)	100 (+)	40.22	7.05 ± 0.13
C4	200 (+)	100 (+)	50.31	4.99 ± 0.19
C5	120 (-)	90 (0)	40.66	7.23 ± 0.11
C6	200 (+)	90 (0)	45.48	5.86 ± 0.11
C7	160 (0)	80 (-)	58.50	7.06 ± 0.10
C8	160 (0)	100 (+)	52.94	6.33 ± 0.11
C9	160 (0)	90 (0)	62.88	7.03 ± 0.11
C10	160 (0)	90 (0)	60.54	6.50 ± 0.10
C11	160 (0)	90 (0)	61.42	6.66 ± 0.12
C12	160 (0)	90 (0)	64.49	6.32 ± 0.11
C13	160 (0)	90 (0)	53.96	6.59 ± 0.17

The application of *P*-values is to check the significance of each of the coefficients for essentially understanding the pattern of the mutual interactions between the test variables. To imply the result of %yield, both the first order mainly affected to inlet temperature (A) and second order mainly affected to inlet temperature (A^2) result from their *P*-values = 0.0337 and 0.0006, respectively. Consequently, they were the most significant effects ($P < 0.05$) (Table 12). For moisture content, the first order main effect of inlet temperature and % aspirator were a significant effect by referring from its *P*-value < 0.0001 and *P*-value = 0.0008 ($P < 0.05$), respectively (Table 13).

Table 12 ANOVA for response surface quadratic model of % yield

Source of variations	Sum of squares	df	Mean square	F-value	Probability P (> F)
Model	1026.49	5	205.30	10.83	0.0034*
A-Inlet temp	131.40	1	131.40	6.93	0.0337*
B-%Aspirator	3.42	1	3.42	0.18	0.6835
AB	2.36	1	2.36	0.12	0.7347
A^2	652.10	1	652.10	34.42	0.0006*
B^2	20.36	1	20.36	1.07	0.3344
Residual	132.63	7	18.95		
Lack of Fit	67.56	3	22.52	1.38	0.3689**
Pure Error	65.08	4	16.27		
Corrected Total	1159.13	12			

* Significant at *P value* = 0.05
** Not significant at *P value* = 0.05
*** R-Squared = 0.8125

Table 13 ANOVA for linear model of %moisture content

Source of variations	Sum of squares	df	Mean square	F-value	Probability P (> F)
Model	5.62	2	2.81	58.08	< 0.0001*
A-Inlet temp	4.52	1	4.52	93.42	< 0.0001*
B-%Aspirator	1.10	1	1.10	22.73	0.0008*
Residual	0.48	10	0.048		
Lack of Fit	0.21	6	0.035	0.51	0.7819**
Pure Error	0.28	4	0.069		
Corrected Total	6.11	12			

* Significant at *P value* = 0.05
** Not significant at *P value* = 0.05
*** R-Squared = 0.6763

Table 14 Model Summary Statistics of %yield and % moisture content

Responses	Std. Dev.	R-Squared	Adjusted R-Squared	Predicted R-Squared	PRESS
%Yield					
Quadratic	4.35	0.8856	0.8038	0.3672	733.46
%Moisture content					
Linear	0.22	0.9207	0.9049	0.8707	0.79

To apply multiple regression analysis on the experiment data, the experiment results of the face centered design were fitted with a second-order polynomial equation of %yield and linear equation of %moisture content. The coefficients of regression equation associated to the responses to the experimental variables and interactions are represented in Table 15.

Table 15 Coefficients of the regression equation linking the responses to the experimental factors and major interactions (coded units)

Responses	Parameters	Coefficients
%Yield	Intercept	60.02
	A-Inlet temp	4.68
	B-%Aspirator	0.76
	AB	-0.77
	A^2	-15.37
	B^2	-2.72
%Moisture content	Intercept	6.58
	A-Inlet temp	-0.87
	B-%Aspirator	-0.43

Thus the mathmatical regression model for % yield and %moisture content fitted in the coded factors were given as following:

$$\%\text{Yield} = 60.02 + (4.68\times A) + (0.76\times B) - (0.77\times AB) - (15.37\times A^2) - (2.72\times B^2) \quad \text{.....(1)}$$

$$\%\text{Moisture content} = 6.58 - (0.87\times A) - (0.43\times B) \quad \text{.....(2)}$$

A and B were the coded values of the test variables;

A: inlet temperature

B: %aspirator

According to the final equation in terms of coded parameters, it may be shown in the equation (1) that increasing of inlet temperature (A) enhanced the %yield while the %aspirator (B) has not significantly affected on %yield (Table15). The results revealed that increasing inlet temperature upto 180°C increased %yield. From higher than 180 °C the opposite results obtained. The reason might be attributed to the compositions of spray drying solution such as carbohydrates that might be stricky as exposed to high temperature. The % yield of different value of the variables could be predicted from the response surface plot (quadratic model).

For %moisture content, the first order main effect of inlet temperature (A) and %aspirator (B) was a significant effect. It was suggested that an increase in inlet temperature and %aspirator were a direct decrease in residual moisture in the products. This finding was consistent with previous research in that the moisture content was decreased with an increased inlet temperature and aspirator capacity (Stahl et al., 2002). The moisture content was possibly forecasted from linear regression plot (linear model). Figure 19 shows the response surface plot for %yield and linear regression plot for %moisture content, respectively.

The normal probability plot of the resdiuals is an vital diagnostic tool for the detection and explaination of the systematic departures from the assumptions to support errors normally distributed and no affected to each other whose variances are homogeneous (Myers and Montgomery, 2002). Figure 20 are the plots of normal probability of experiment results. The normal probability plot of the "Studentised" residuals indicates almost no violation of the assumptions outlying the analyses.

Based on the two models obtained, a graphical optimization was also conducted the hardness of the Design-Expert version 7.1 statistical software. Recall, the main objective was the maximization of %yield and the minimization of %moisture content. The selection of conditions to overlay plot ranged from 120-200 °C and 80-100% for inlet temperature and %aspirator, respectively. The method basically consisted of overlaying the curves of the models according to the criteria imposed that was to higher %yield as possible and lower %moisture content as possible .

By considering the inverse relationship between %yield and %moisture content, the attained overlaying plot displayed a non-shaded area (white area) where both criterias imposed were satisfied (Figure 21). Hence, a point was selected on the graph (marked by the square). This point was assigned as optimal point and corresponded to 178°C of inlet temperature and 100% of aspirator. Under such conditions, the model predicted 56.90 %yield (a variation of = 49.97 – 63.83% being possible) and 5.77 %moisture content (a variation of = 5.52 – 6.33% being possible) in the confidence range of 95%.

The statistical interpretation of the results concerning both yield and moisture content using the response surface methodology led us to the choice of optimal operating condition. These parameters had to maximize yields while reducing moisture contents.

To confirm the result, three batches were produced using the optimal conditions to validate the fabrication process (Table 16).

According to Table 17, the observed means and standard deviations of the responsed obtained for yield and moisture content were found to be 50.40±4.13% and 6.07±0.37%, respectively. They were in range of the prediction intervals at 95% confidence level. These results can be concluded that the model fitted the experimental data well and described the region studied well

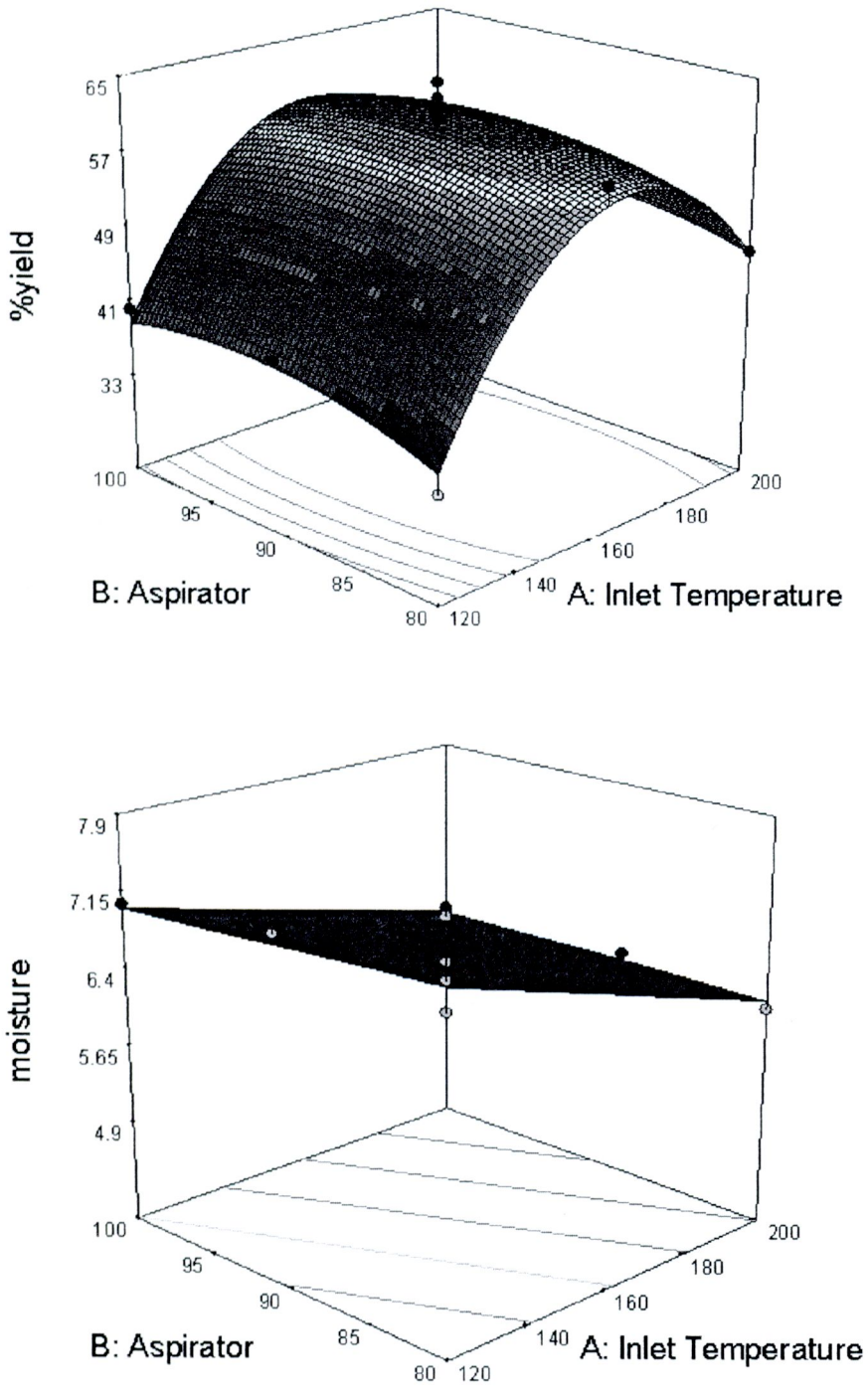

Figure 19 Response surface plot of % yield and linear regression plot of %moisture content; (a) response surface plot of % yield, (b) linear regression plot of %moisture content

Normal plot residuals of %yield results

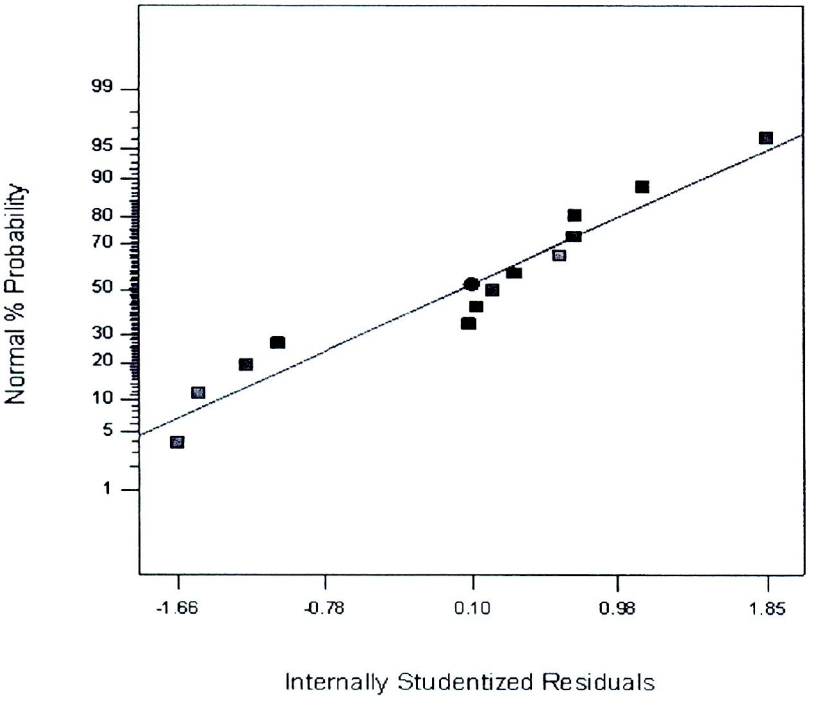

Normal plot residuals of %moisture content results

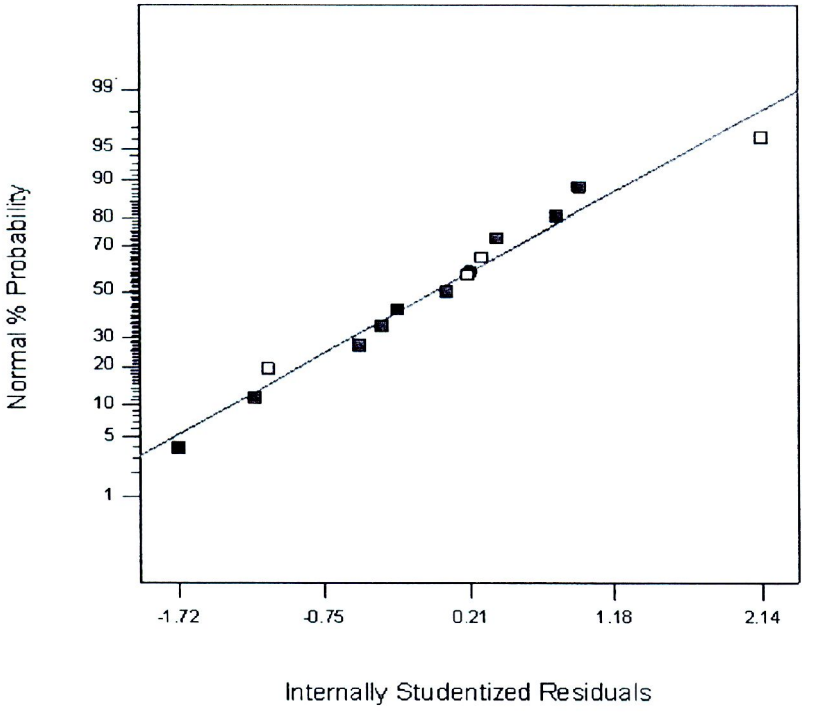

Figure 20 The normal probability plots of the %yield and %moisture content;

(a) The normal probability plot of the %yield results

(b) The normal probability plot of the %moisture content results

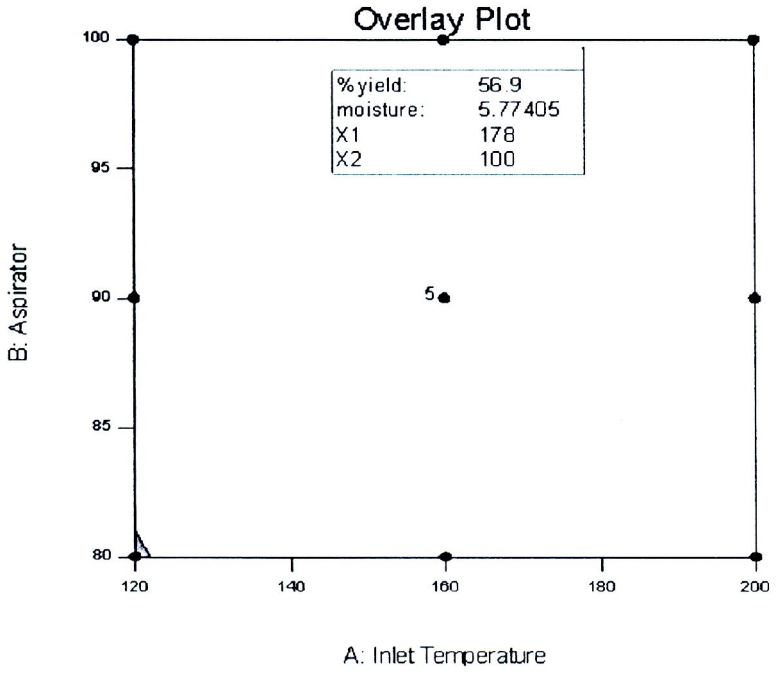

Figure 21 The optimum region by overlay plot of two responses (%yield and %moisture content) evaluated as a function of inlet temperature and %aspirator

Table 16 The optimum region by overlay plot of two parameters and the observed responses

Code	Factor		Responses	
	Inlet temperature (°C)	**% Aspirator**	**%yield**	**%moisture**
O1	178	100	52.49	6.25
O2	178	100	53.06	6.32
O3	178	100	45.84	5.65

Table 17 Observed responses and 95% CI (confidence interval) of optimization spray dried condition

Responses	Values		
	%Observed	%Predicted	95% confidence intervals
Total yield (%)	50.40 ± 4.13	56.90	49.97 – 63.83
Moisture content (%)	6.07 ± 0.37	5.77	5.52 – 6.33

Figure 22 was displayed the optimal xyloglucan spray dried powder obtained as fine particles with whitish color and powder bulkiness.

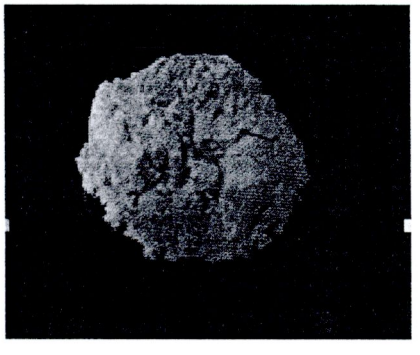

Figure 22 Xyloglucan spray dried powder of optimal spray dried condition

2. Morphology of xyloglucan spray dried powders

The shape and surface topography of the xyloglucan spray dried particles were found to be affected by the spray drying condition. The observation of size, shape and surface topography were done by scanning electron microscopy (SEM). Figure 23 showed the scanning electron photomicrographs of spray dried particles obtained from varied conditions. The particle topography of all conditions were all very small spheres. Some condition such as C8 and C9 gave shrunk particles. At the higher magnification (×10,000), the particles spray dried from the optimal condition (Figure 23i) showed rough surfaces. The rough surface of particles probably was result from propylene glycol, one of the components in preservative (Sepicide® HB) added in spray drying solution. To confirm the postulation, the spray drying solution without preservative (0.5% Sepicide® HB) was spray dried by the same optimal condition. Consequently, it was found that the surface topography of the spray dried particle was

smooth (Figure 23j). From the results, it might be postulated that the shrinkage of particle surfaces was related to the presence of Sepicide® HB. Sepicide® HB consisted of phenoxyethanol, methylparaben, ethylparaben, propylparaben and butylparaben in propylene glycol. The solvent effect of propylene glycol might affect the evaporation of water from the spraying droplets. This finding also agreement with the previous research that solvent had influenced on particle size and morphology of ZnO preparation (Kanade et al., 2006).

3. Particle size and size distribution

In this study, the average particle size (D [4, 3]) and particle size distribution (Span value) were determined and compared between different inlet temperature and %aspirator values of xyloglucan spray dried particles. The particle sizes ranged from 8.26±0.02 to 10.87±0.06μm and the span values ranged from 2.33±0.01 to 2.64±0.02μm (Table 18). It was noticed that the particle size obtained from SEM, this method provided the same range of that obtained from light scattering method. As has been shown, an increase in inlet temperature could trended to increase the particle size whereas increasing %aspirator decreased the paticle size. The correlation between the particle size and the inlet temperature was in agreement with the previous study that spray-dried insulin intended for inhalation (Stahl et al., 2002).

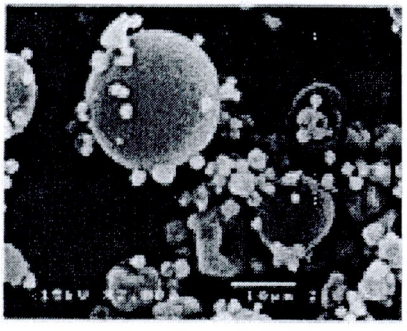

(× 2000)

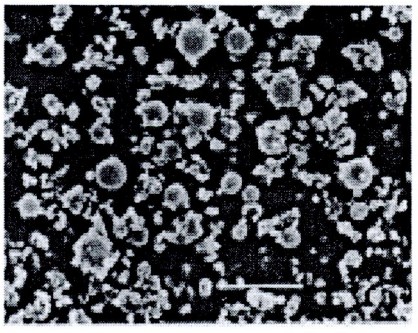

(×500)

(a) C1

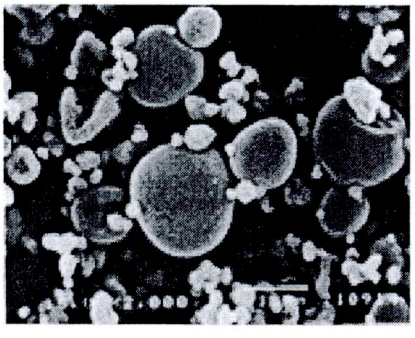

(× 2000)

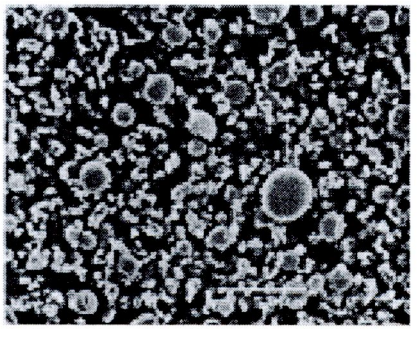

(×500)

(b) C2

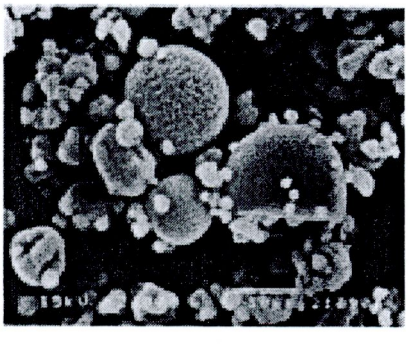

(× 2000)

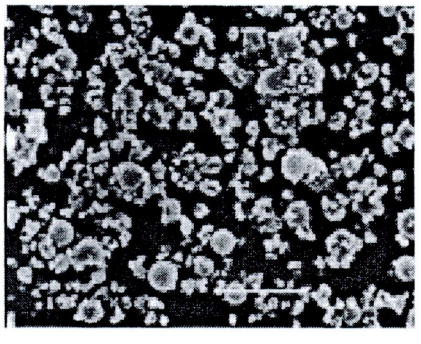

(×500)

(c) C3

Figure 23 Scanning electron photomicrographs of xyloglucan spray dried powder from experimental design

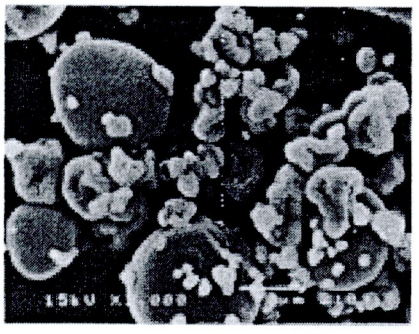

(× 2000)

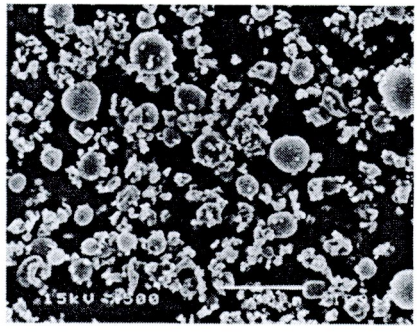

(×500)

(d) C4

(× 2000)

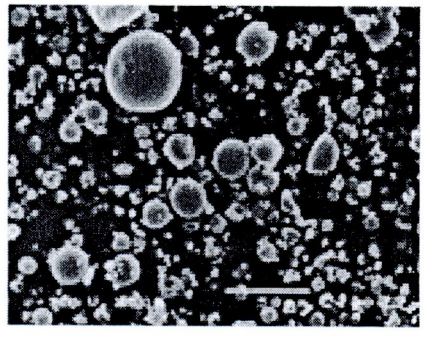

(×500)

(e) C5

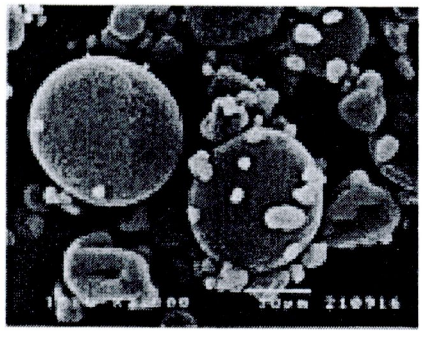

(× 2000)

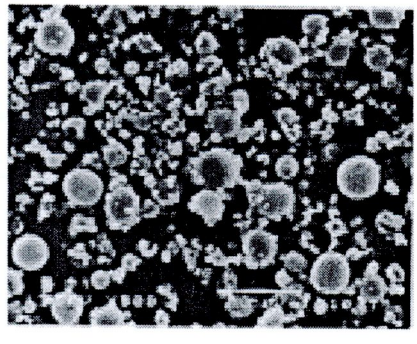

(×500)

(f) C6

Figure 23 Scanning electron photomicrographs of xyloglucan spray dried powder from experimental design (continued)

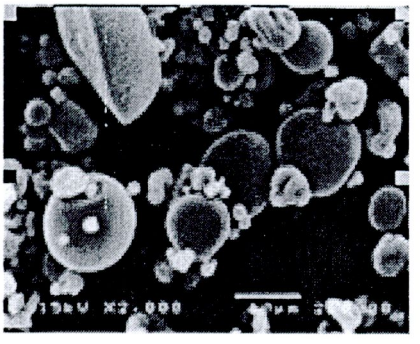

(× 2000)

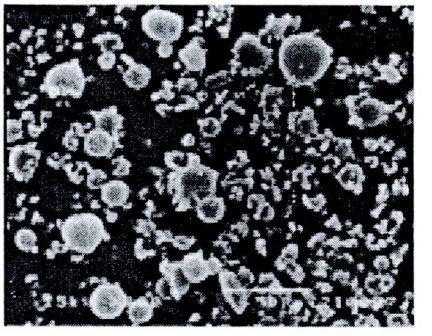

(×500)

(g) C7

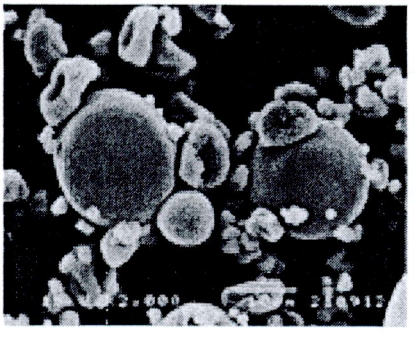

(× 2000)

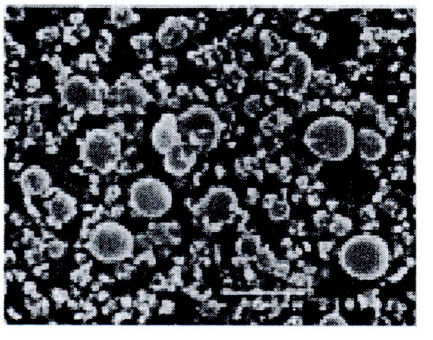

(×500)

(h) C8

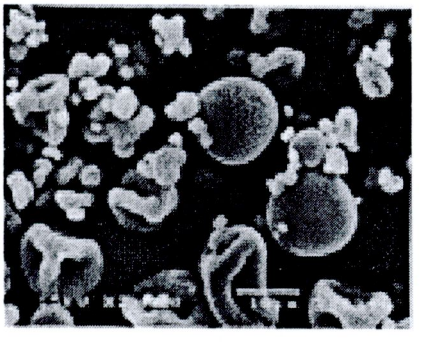

(× 2000)

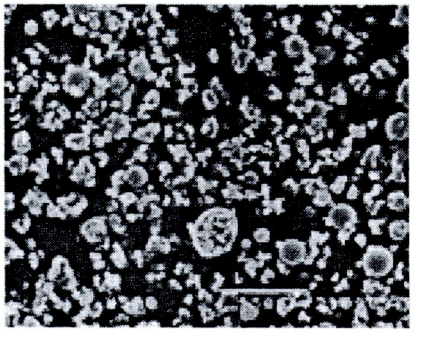

(×500)

(i) C9

Figure 23 Scanning electron photomicrographs of xyloglucan spray dried powder from experimental design (continued)

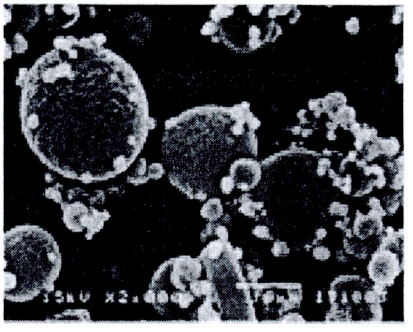

(× 2000)

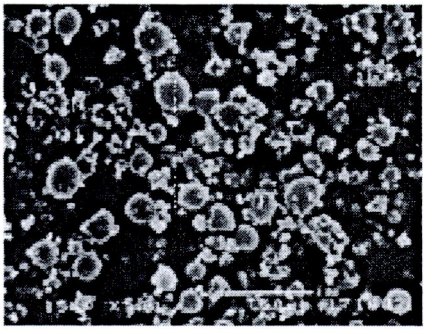

(×500)

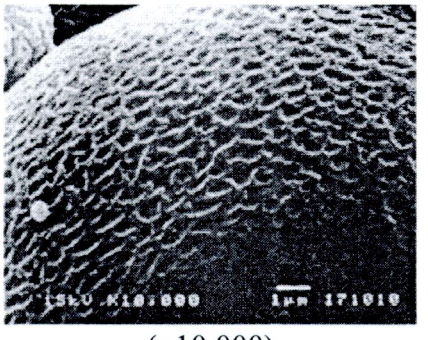

(×10,000)

(i) Optimum sample

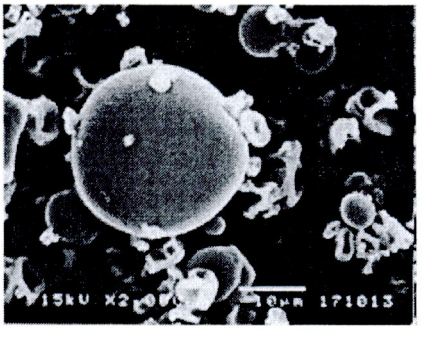

(× 2000)

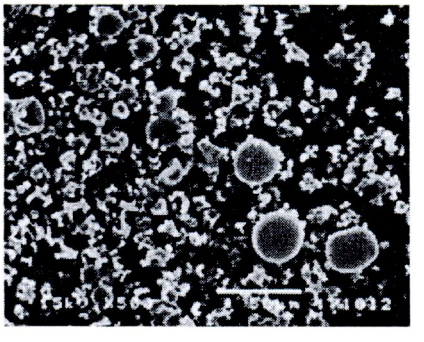

(×500)

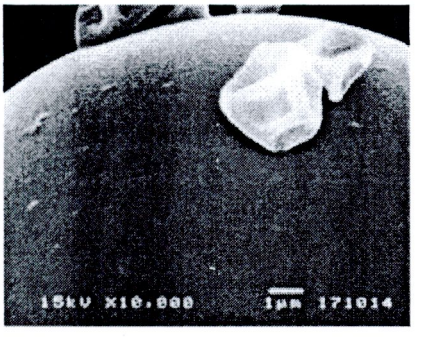

(× 10,000)

(j) Optimum sample without preservative

Figure 23 Scanning electron photomicrographs of xyloglucan spray dried powder from experimental design (continued)

Table 18 The particle size distributions of the xyloglucan spray dried particles (mean ± SD; n=3)

Factor		Average particle size	
Inlet temperature (°C)	**% Aspirator**	**D [4, 3] ± SD (μm)**	**Span ± SD**
120	80	11.15 ± 0.04	2.43 ± 0.02
200	80	10.86 ± 0.05	2.63 ± 0.01
120	100	8.26 ± 0.02	2.60 ± 0.02
200	100	9.66 ± 0.02	2.33 ± 0.01
120	90	9.16 ± 0.06	2.37 ± 0.03
200	90	10.40 ± 0.03	2.47 ± 0.01
160	80	9.94 ± 0.06	2.64 ± 0.02
160	100	9.66 ± 0.11	2.45 ± 0.01
160	90	9.45 ± 0.14	2.59 ± 0.01
178	100	10.87 ± 0.06	2.47 ± 0.01

C. Evaluation of physicochemical properties of xyloglucan powder from tamarind seeds

Xyloglucan powder was analyzed for the xyloglucan content by HPLC method (Appendix D) was exhibited that the content was 42.30±0.50%. There are 8 examined physicochemical properties of xyloglucan powder from tamarind seed in this study.

1. pH

The pH value of xyloglucan powder from tamarind seed was 7.83±0.19. This was in agreement with the report by **Megazyme International Ireland Ltd** in that the pH of xyloglucan standard **ranged neutral.**

2. Solubility in water

The solubility value in water of xyloglucan powder from tamarind seed was 6.28±0.08 mg/ml. This finding was lower than the data reported by **Megazyme International Ireland Ltd** in that the solubility value in hot water of standard **was 10 mg/ml. This might be due to the differences of temperature of water in the studies and in purity of the spray dried powder obtained in this study from the**

commercial standard. In this study, the xyloglucan content was approximately 42% **and also composed of proteins, fats and other carbohydrates.**

3. Viscosity and rheology property

Table 19 displays the viscosity values and rheology properties of 1%, 1.5% and 2% w/w of xyloglucan powder from tamarind seed in purified water. The viscosity of 1%, 1.5% and 2% w/w of xyloglucan powder from tamarind seed ranged from 39.46 ± 0.85 to 168.06 ± 1.83. Xyloglucan solution of all concentrations exhibited typical Pseudoplastic flow (Figure 24). However, the result conformed with the report by Sims et al (1998) that xyloglucan solution was viscous and displayed non-Newtonian behavior. This was conflicting with the previous report that xyloglucan solution exhibited typical Newtonian flow (13th European Carbohydrate Symposium, 2005). The explanation might be possibly resulted the difference of purity of xyloglucan sample.

Table 19 The viscosity values and rheology properties of 1, 1.5 and 2%w/v of xyloglucan powder from tamarind seed (mean ± SD)

%w/w of Xyloglucan extract	Viscosity (mPa)	Rheology
1%	39.46 ± 0.85	Pseudoplastic flow
1.5%	93.68 ± 0.91	Pseudoplastic flow
2%	168.06 ± 1.83	Pseudoplastic flow

4. Incompatibility of xyloglucan and ethanol

The study of the incompatibility of xyloglucan and ethanol was operated since ethanol was used in the solubilizing system of *Centella* extract in film formulation in the next study. Whereas, Suttananta (1986) and Tine et al. (2006) reported that xyloglucan could be precipitated by ethanol. In this study, incompatibility of xyloglucan and ethanol of 1% w/v of xyloglucan powder from tamarind seed was determined. Table 20 displays the percentages of remained and reduced xyloglucan after added with ethanol. The percentages of remained and reduced xyloglucan after added with 1-5% ethanol ranged from 82.53±1.60 to 98.51±1.53 and 1.49-17.47,

respectively. As the results, it was shown that the solution of xyloglucan powder form tamarind seed was incompatibility with ethanol in the range 1-5%.

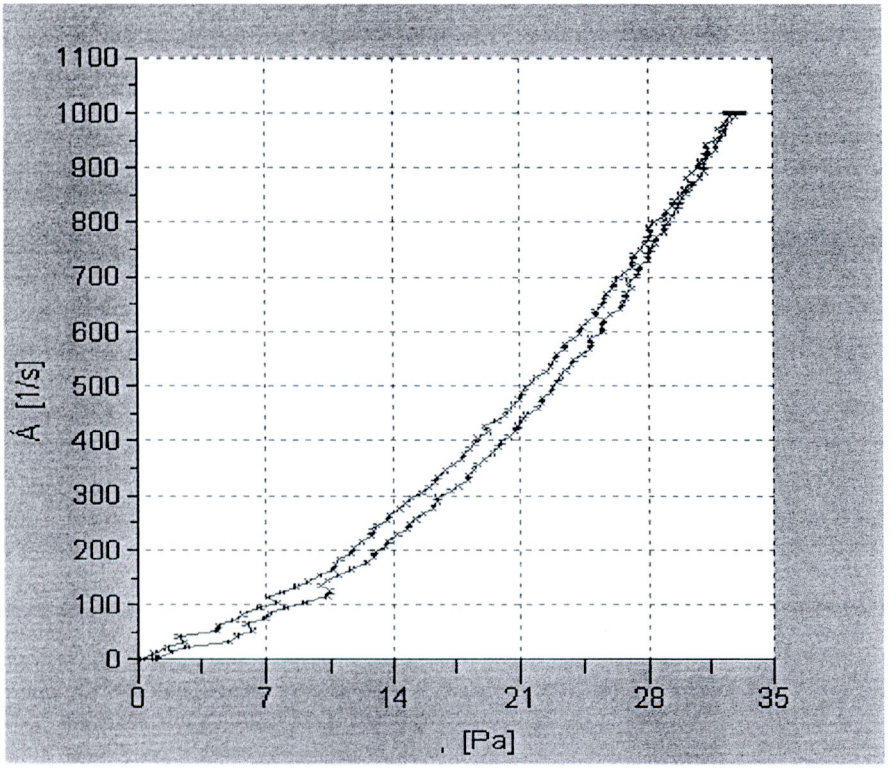

Figure 24 Rheogram of 1%w/v xyloglucan spray dried powder

Table 20 The percentage of remained and reduced xyloglucan after added with ethanol (Mean ± SD)

%Ethanol	%Remained xyloglucan	% Xyloglucan loss
0	100	-
1	98.51 ± 1.53	1.49
2	95.14 ± 0.68	4.86
3	92.38 ± 1.46	7.62
4	86.16 ± 1.86	13.14
5	82.53 ± 1.60	17.47

5. Differential scanning calorimetric thermograms

The DSC thermograms of standard xyloglucan and xyloglucan powder from tamarind seed are shown in Figures 25. It was found that there were broad endotherms in both standard xyloglucan and xyloglucan powder (40-120°C). This might be caused by the loss of moisture absorbed in the standard xyloglucan and xyloglucan powder. From the diffactogram, it was clear that both standard xyloglucan and xyloglucan spray dried powders showed no melting endothrem. However, at high temperatures than 290°C, it was noticed that standard xyloglucan and xyloglucan spray dried powders showed degradation. It might conclude that xyloglucan spray dried powder existed in an amorphous state.

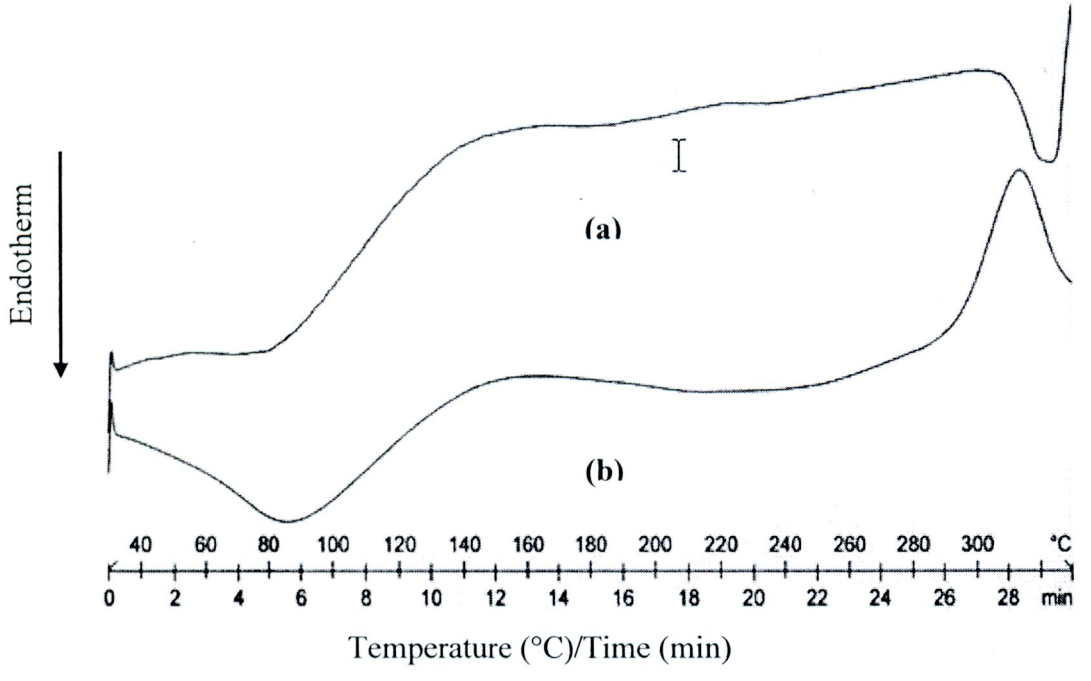

Figure 25 The DSC thermograms of standard xyloglucan and xyloglucan powder from tamarind seed

(a) Standard xyloglucan

(b) Xyloglucan powder from tamarind seed

6. Powder X-ray Diffractometry

Powder X-ray diffractometry may be used to detect crystallinity in the solid state. Figure 26 shows the X-ray diffractograms of standard xyloglucan and xyloglucan powder from tamarind seed. The diffractograms of standard xyloglucan and xyloglucan powder did not present intense diffraction peaks so, the standard xyloglucan and tamarind seed xyloglucan existed in an amorphous state. The result confirmed the observation that obtained from the DSC thermograms.

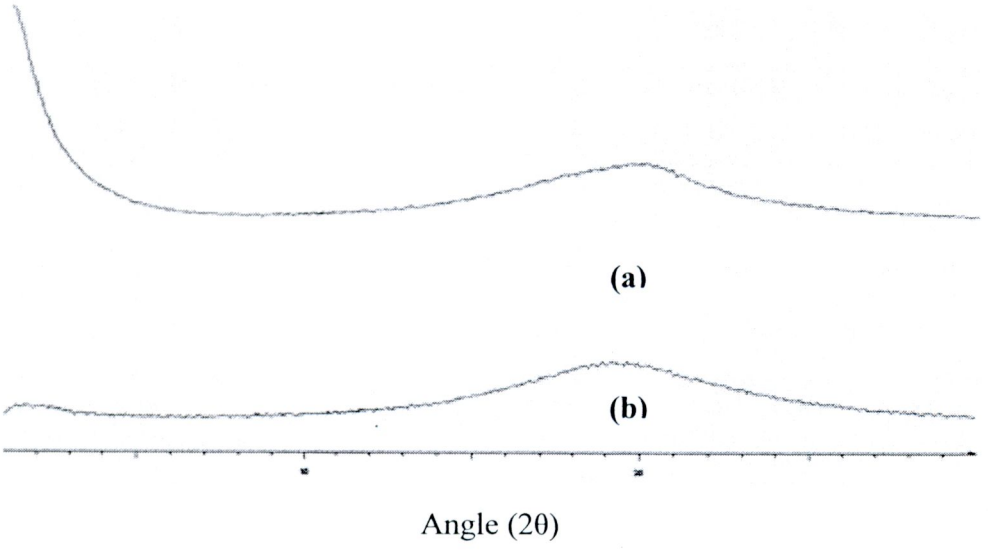

Figure 26 X-ray diffractograms of standard xyloglucan and xyloglucan powder from tamarind seed

(a) Standard xyloglucan

(b) Xyloglucan powder from tamarind seed

7. Particle size and size distribution

Figure 27 displayed scanning electron microscopy (SEM) of xyloglucan powder from tamarind seed. Topography of xyloglucan powder were very small spheres some with smooth surfaced but some were shrunk. The average particle size (D [4, 3]) and particle size distribution (Span value) of xyloglucan powder were 11.49 ± 0.11 and 2.47 ± 0.02, respectively.

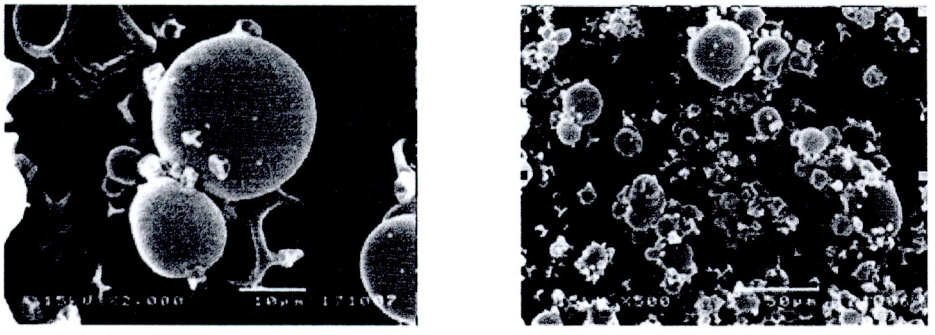

Figure 27 Scanning electron photomicrographs of xyloglucan powder

D. Evaluation of film formulations prepared from xyloglucan spray dried powders containing *Centella asiatica* extract

1. Physical Appearances

All films prepared from xyloglucan spray dried powder were pale brown in color, transparent, smooth and flexible film (Figure 28). The thickness and weight of the films of 1×1 cm^2 were in the range of 0.03-0.07 mm. and 6.90±0.23-13.07±0.20 mg, respectively (Table 21). Films formulation prepared from tamarind seed containing *Centella asiatica* extract, the thickness and film weight were 0.047±0.006 mm and 12.71±0.22 mg, respectively. This showed that the addition of *Centella* extract did not affect the physical appearance of the film.

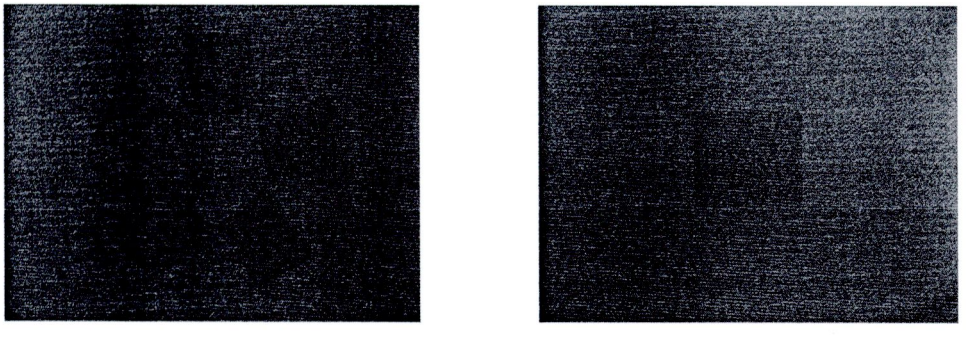

(a) **(b)**

Figure 28 The appearance of films

(a) films prepared from xyloglucan powder

(b) films prepared from xyloglucan powder containing *Centella asiatica* extract

Table 21 The thickness and film weight data of films (mean ± SD)

Formulation	Thick (mm)	Film weight (mg)
F1	0.05 ± 0.00	11.54 ± 0.39
F2	0.06 ± 0.00	11.23 ± 0.31
F3	0.03 ± 0.00	14.99 ± 0.33
F4	0.03 ± 0.00	4.81 ± 0.24
F5	0.03 ± 0.00	9.72 ± 0.32
F6	0.06 ± 0.00	8.73 ± 0.15
F7	0.06 ± 0.00	7.72 ± 0.25
F8	0.07 ± 0.00	13.07 ± 0.20
F9	0.07 ± 0.00	6.90 ± 0.23
F10	0.06 ± 0.00	10.44 ± 0.35
F11	0.05 ± 0.00	9.58 ± 0.38
F12	0.04 ± 0.00	9.07 ± 0.55
F13	0.04 ± 0.00	9.36 ± 0.36
F14	0.05 ± 0.00	7.87 ± 0.20
F15	0.04 ± 0.00	8.21 ± 0.34
Film with extract	0.05 ± 0.006	12.71 ± 0.22

2. Determination of adhesive force of film formulations

The adhesive force evaluated at a predetermined contact time was investigated using porcine skin as a model membrane. The force of maximum detachment force (force of adhesive) and work of adhesive as two parameters were used to evaluate the adhesive properties of films. The results in Table 22 show the adhesive force data of films.

The adhesive forces of films were in range 1.566±0.74-21.160±15.49 N/cm^2. As the results, it showed that the adhesive force of F6 was the highest value in all film formulation. In this study, F6 was selected to prepare the film formulation containing *Centella asiatica* extract. The adhesive force of film containing *Centella asiatica* extract was 3.703±1.11 N/cm^2. It was surprising that the incorporation of *Centella*

asiatica extract, the adhesive force of film much decreased. This effect might be resulted from the dispersing of *Centella* extract in film formulation that interfered the adhesive force between the xyloglucan film and porcine skin. It was found from the experimental data, that the standard deviation was high. The high standard derivation was possibly occurred from biological variation of porcine skin using in the test and xyloglucan powder from tamarind seed, which was the natural product resulting high variation, used in film formation.

3. Determination of mechanical properties of films and films formulation

A tensile testing gave an indication of the strength and elasticity of the film reflected by the following parameters: tensile strength, elongation and Young's modulus. Tensile strength or more accurately the ultimate tensile strength is the maximum tensile strength that a film can sustain. Elongation demonstrates the performance of a film to stretch before breaking. Young's modulus or the modulus of elasticity is the ratio of stress to strain over the linear part of stress–strain curve, and it is a measure of film stiffness (Ozdemir and Floros, 2008). It was found that a hard and tough film is greatly appropriate for the intended application as drug delivery systems for the skin. Their flexibility was sufficient for the movements of the skin without breaking, however, at the same time an increased strength for a prevention abrasion of the film caused for example by contact with clothing was apparent (Schroeder et al., 2007). The classification of films according to the value of tensile strength and %elongation is shown in Table 23.

The data of tensile strength, elongation, work of failure and Young's modulus of the films are displayed in Table 24. The tensile strength, elongation, work of failure and Young's modulus of the films were in range 2.77±0.23 to 15.45±3.38 MPa, 87.92±13.38 to 568.60±50.62%, 5.16±0.77 to 28.72±8.66 mJ and 2.48± 0.22 to 22.33±7.03 MPa, respectively. It was found from the experimental data, that the standard deviations were high. The high standard deviations might possibly occur from xyloglucan powder from tamarind seed, which was the natural product resulting high variation.

Table 22 The force of adhesive data of films. (mean ± SD)

Formulation	Force of adhesion (N/cm^2)
F1	3.366 ± 0.02
F2	2.616 ± 0.71
F3	19.560 ± 7.77
F4	6.029 ± 2.58
F5	7.156 ± 4.81
F6	21.160 ± 15.49
F7	3.704 ± 0.83
F8	2.312 ± 2.42
F9	1.566 ± 0.74
F10	13.480± 10.66
F11	2.212 ± 0.72
F12	3.659 ± 0.97
F13	3.029 ± 1.24
F14	1.733 ± 0.18
F15	3.393 ± 1.54
Film with extract	3.703 ± 1.11

Table 23 The values of tensile strength and %elongation of classification of film (Schroeder et al., 2007).

Typical film	Value	
	Tensile Strength (MPa)	%Elongation
Soft and weak	low	low
Hard and brittle	high	low
Soft and tough	low	high
Hard and tough	high	high

F5 and F6 were composed of 4%w/w of sorbitol solution and 2% w/w glycerin but the percentage amounts of xyloglucan powder were different by 1 and 2% w/w, respectively. By comparison, an increase in % xyloglucan powder resulted in an increase in tensile strength of film but a decrease in Young's modulus and no difference of %elongation. Consequently, increasing %xyloglucan powder enabled film to be harder and tougher.

To compare F9 and F10 which contained different %glycerin, 0 and 4%, respectively but had similar compositions of xyloglucan powder and sorbitol solution, it was found that an increase in % glycerin resulted in lower tensile strength, lower Young's modulus and higher %elongation. As a result, film is softer and tougher when increasing %glycerin.

To compare F7 and F8 which had different percentage amounts sorbitol solution by 2 and 6%, respectively but had similar composition of xyloglucan powder and glycerin, it was found that an increase in sorbitol solution resulted in higher tensile strength, lower %elongation and no difference of Young's modulus. As a result, film is hard and brittle when increasing sorbitol solution.

The tensile strength, elongation, work of failure and Young's modulus of the films containing *Centella asiatica* extract were 15.11±2.32, 232.73±17.50, 12.24±2.19 and 5.81±1.18, respectively. By comparison between F6 and the film containing *Centella asiatica* extract, it was found that adding *Centella asiatica* extract resulted in higher tensile strength, lower %elongation and no difference of Young's modulus. As a result, the film is harder. The previous research reported that a hard and tough film is greatly appropriate for the intended application as drug delivery systems for the skin (Schroeder et al., 2007). So, F6 might be appropriate film formulation.

Table 24 Mechanical propertydata of film formulations and film containing *Centella asiatica* extract (mean ± SD)

Formulation	Tensile Strength (MPa)	%Elongation	Work of failure (mJ)	E-Mod (MPa)
F1	15.45 ± 3.38	176.84 ± 13.98	10.56 ± 2.78	8.09 ± 1.67
F2	4.74 ± 0.81	375.20 ± 42.75	13.88 ± 3.32	2.96 ± 0.39
F3	4.02 ± 1.32	491.30 ± 49.31	9.61 ± 2.78	4.90 ± 2.04
F4	14.50 ± 0.56	128.10 ± 14.78	5.16 ± 0.77	17.92 ± 4.09
F5	4.73 ± 0.49	360.80 ± 14.04	7.25 ± 0.82	5.88 ± 1.13
F6	12.03 ± 0.91	357.60 ± 73.39	23.67 ± 6.76	4.46 ± 0.31
F7	3.84 ± 0.57	547.10 ± 56.45	20.35 ± 4.87	3.44 ± 0.34
F8	6.90 ± 1.95	164.83 ± 19.544	5.94 ± 1.65	3.83 ± 0.48
F9	10.70 ± 1.76	87.92 ± 13.38	5.93 ± 1.50	22.33 ± 7.03
F10	2.77 ± 0.23	494.10 ± 64.49	11.95 ± 2.88	2.48 ± 0.22
F11	7.39 ± 2.52	561.30 ± 62.10	28.72 ± 8.66	5.16 ± 1.65
F12	3.61 ± 0.80	525.00 ± 27.82	15.08 ± 1.11	3.80 ± 0.73
F13	6.85 ± 2.20	568.60 ± 50.62	25.18 ± 4.630	5.42 ± 0.78
F14	5.79 ± 0.62	513.50 ± 6.47	20.66 ± 3.32	3.99 ± 0.42
F15	7.04 ± 2.56	503.30 ± 117.85	23.52 ± 10.77	6.84 ± 3.43
Film containing *Centella asiatica*	15.11 ± 2.32	232.73 ± 17.50	12.24 ± 2.19	5.81 ± 1.18

4. Differential scanning calorimetric thermograms

The DSC thermograms of *Centella asiatica* extract, film prepared from xyloglucan powder and film prepared from xyloglucan powder containing *Centella asiatica* extract were depicted in Figure 29. The DSC thermogram of the *Centella* extract showed the endothermic melting peaks at 238°C. The result showed that there was at least one component in *Centella asiatica* extract was in crystalline form. Film prepared from xyloglucan powder exhibited no melting peak. In addition, it was found that the endothermic peak corresponding to *Centella* extract melting was not observed in the thermograms of film formulation containing *Centella asiatica* extract. The

results might be explained that the *Centella* extract in film formulation was uniformly dispersed in an amorphous state.

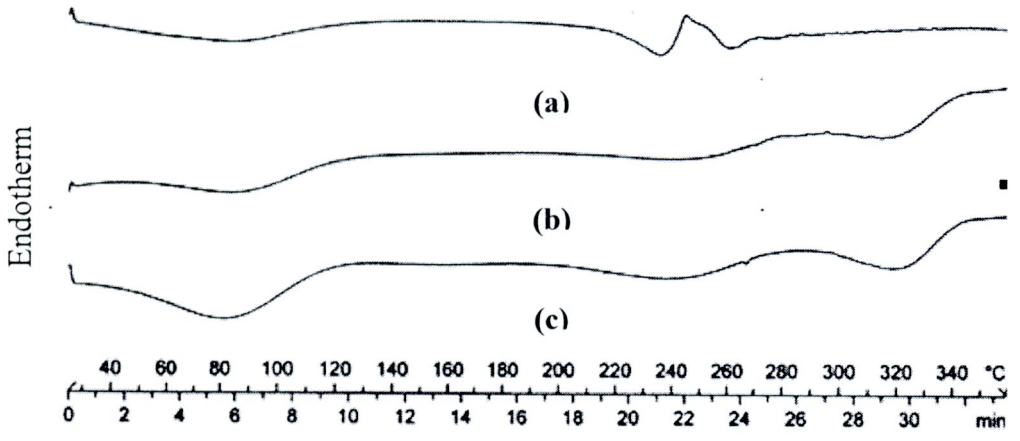

Figure 29 The DSC thermograms of *Centella asiatica* extract, film prepared from xyloglucan powder and film prepared from xyloglucan powder containing *Centella asiatica* extract;

(a) *Centella asiatica* extract

(b) Film prepared from xyloglucan powder

(c) Film prepared from xyloglucan powder containing *Centella asiatica* extract

5. Powder X-ray Diffractometry

The x-ray diffractograms of *Centella asiatica* extract, film prepared from xyloglucan powder and film prepared from xyloglucan powder containing *Centella asiatica* extract are shown in Figure 30.

The diffractograms of *Centella asiatica* extract exhibited a series of intense diffraction peaks, which indicative of their crystalline characteristic. The prominent peaks of x-ray diffractogram of *Centella asiatica* extract were particularly observed at 5.11°, 13.88°, 14.24° and 15.29°, respectively. Whereas the diffractograms of film prepared from xyloglucan powder and film prepared from xyloglucan powder containing *Centella asiatica* extract did not present intense diffraction peak. This result conformed to the DSC thermograms (Figure 28). It might be concluded that the

Centella extract was molecularly dispersed with film prepared from xyloglucan powder or existed in an amorphous state.

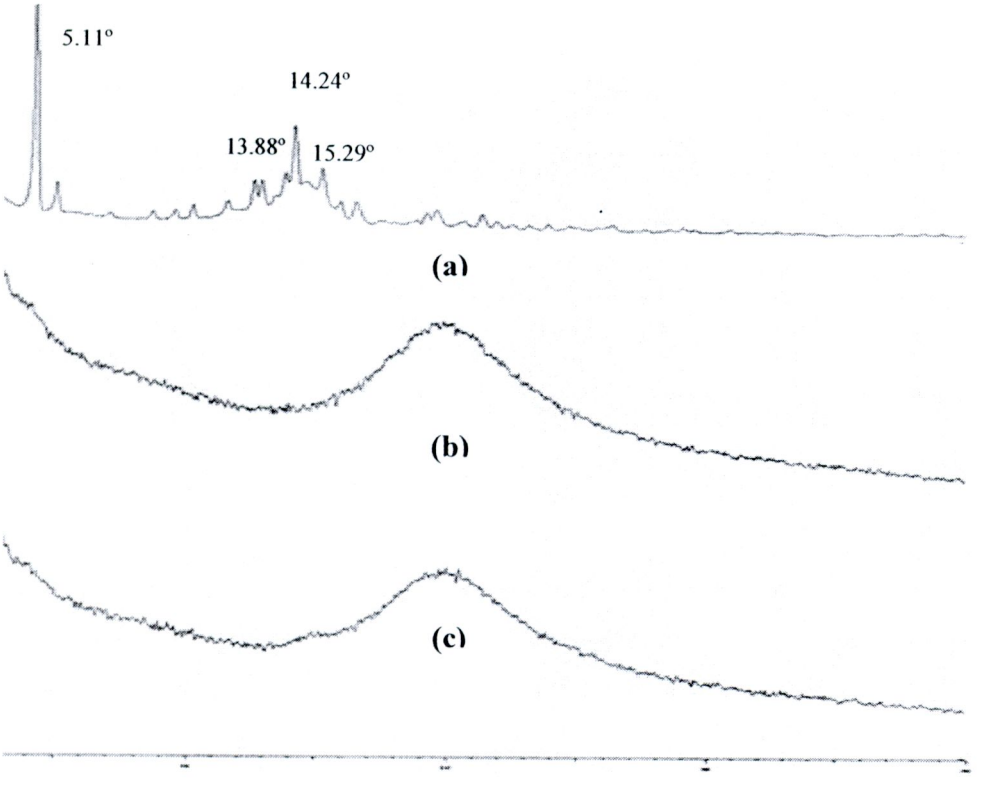

Figure 30 X-ray diffractograms of *Centella asiatica* extract, film prepared from xyloglucan powder and film prepared from xyloglucan powder containing *Centella asiatica* extract;

(a) *Centella asiatica* extract

(b) Film prepared from xyloglucan powder

(c) Film prepared from xyloglucan powder containing *Centella asiatica* extract

6. Release study

Figure 31 and Table 25 presented the release data and release profiles of asiaticoside from film formulation containing *Centella asiatica* extract, respectively. The amount released of asiaticoside was exhibited to be more than 50% within 8 hours from film formulation. The release data over the whole time period were

explained according to the treatment proposed by Higuchi for asiaticoside release from film formulation.

$$Q_t = k_H t^{1/2}$$

where:

Q_t is the amount of drug release at time t

k_H *is* the release rate constants of Higuchi

t is the release time

Plots of the cumulative amount Q_t of drug released versus the square root of time were a short lag period (initial 50–60% release) (Figure 32). The coefficient of determination of the relationship between cumulative amount releases versus square root of time (R^2) of asiaticoside was 0.9861%$h^{-1/2}$. This finding was in agreement with Takahachi et al. (2002) in percutaneous absorption of non-steroidal anti-inflammatory drugs from in situ gelling xyloglucan formulations. Amount of drugs from formulations were released according to Higuchi model.

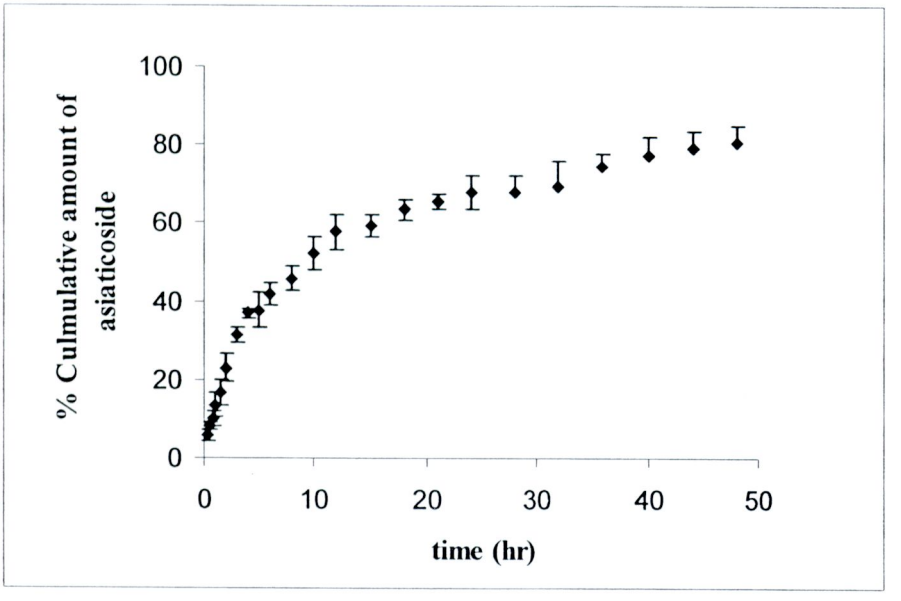

Figure 31 The release profiles of asiaticoside from film formulation

Table 25 The release data of asiaticoside from film formulation (mean ± SD)

Time (hrs)	% Cumulative release of asiaticoside Mean ± SD
0	0
0.25	5.69 ± 1.24
0.5	8.13 ± 1.07
0.75	9.95 ± 2.13
1	13.30 ± 3.08
1.5	16.47 ± 3.28
2	22.91 ± 3.43
3	31.28 ± 2.07
4	36.82 ± 1.27
5	37.63 ± 4.57
6	41.64 ± 2.72
8	45.68 ± 3.22
10	51.95 ± 4.23
12	57.60 ± 4.51
15	59.32 ± 2.90
18	63.34 ± 2.63
21	65.37 ± 2.10
24	67.56 ± 4.28
28	67.54 ± 4.45
32	74.61 ± 2.89
36	77.37 ± 4.54
40	79.01 ± 4.24
48	80.75 ± 3.99

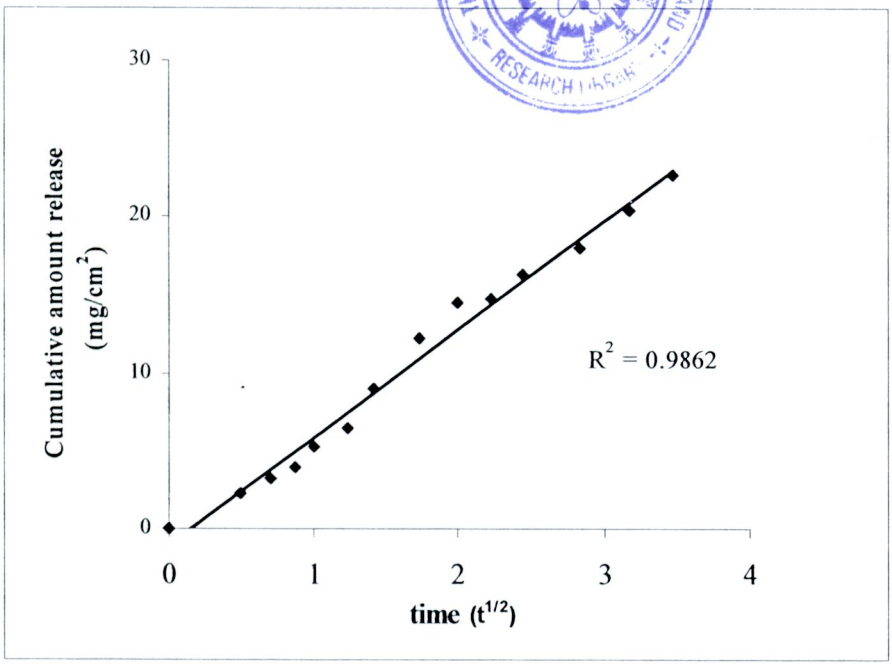

Figure 32 Cumulative releases per unit area, Q, for asiaticoside as a function of square root time from film formulation

7. Permeation study

The permeation study of asiaticoside from film prepared from xyloglucan powder for 24 hours was investigated. The porcine skin was used to be as a model membrance. It found that the asiaticoside which was one of the active components of *Centella asiatica* extract in film formulation could not be detected by HPLC method in the sample taken from the receptor along the study period. The amount asiaticoside inside the porcine skin which, used in the study and film formulation in donor of Franz diffusion cell were determined after the experiment had finished. It found that the percentage of asiaticoside in some porcine skin was so low that it could not be analyzed. The percentage of asiaticoside remaining from film formulation in donor of Franz diffusion cell and porcine skin were 91.14±1.84% and 1.30±1.28%, respectively (Table 26). Although asiaticoside could not permeate through the porcine skin, it could release from film formulation. This result could confirmed that asiaticoside in film formulation could be used for wound healing due to most wounds lost stratum corneum that was barrier.

From the results, there were some possible explanations as follows. This might be occurred because asiaticoside could not permeate through porcine skin. Since there

was about 7.56% of asiaticoside that could not be detected and explained, this might be the limitation of the analysis of asiaticoside in porcine skin. Moreover, it was possible that asiaticoside might decompose and change to asiatic acid which was the other one active component of Centella extract. The HPLC system in the study did not detect and analyse asiatic acid. If this explanation was valid, it was believable that asiaticoside could permeate into the porcine skin and remained present in the form of asiatic acid (Appendix G)

Table 26 The percentage of asiaticoside from film formulations in donor of Franz diffusion cell and porcine skin

Site	% Asiaticoside			Mean	SD
	set 1	set 2	set 3		
Donor's Franz cell	92.51	91.86	89.05	91.14	1.84
Porcine skin	1.33	-	2.56	1.30	1.28

8. Stability study

8.1 Chemical stability study

The stability testing was determined on the film formulation containing *Centella asiatica* extract that had been stored in stressed conditions at the temperature at 40±2 °C and the humidity at 75±5% RH. The amounts of asiaticoside in film prepared from xyloglucan powder was analyzed by HPLC method at the initial time, first, second and third month. The % labeled amount of test preparations which determined at initial time was found to be 93.85%.

From the result, the percentage loss of asiaticoside during 3 months periods was 16.41% (Table 27). The film formulation containing *Centella asiatica* extract were not stable during 3 months periods because the percentage loss of asiaticoside was more than 10% of the initial value (Cartensen, 1990).

It was reported by Hengsawas (2004) that asiaticoside probably be degraded by peroxide, acid and alkaline agents. A degradation of Asiaticoside caused by oxidation mechanism to obtain other compounds while was hydrolyzed by hydronium/hydroxide ion to obtain asiatic acid and sugar moiety, glucose and rhamnose

There were some factors that enhance the degradation of asiaticoside in film formulation containing *Centella asiatica* extract. The first factor, xyloglucan powder

from tamarind seed had hygroscopic property. After the stress condition for 3 periods, asiaticoside was increasingly degraded by hydrolysis due to water content increased in film formulation. The second, the package which used in the study for the film formulation containing *Centella asiatica* extract could not protect the film formulation moisture resulted to hydrolysis.

Table 27 The percentages labeled amount of asiaticoside in film formulation containing *Centella asiatica* extract in stability test (mean ± SD)

Periods	%Loss of asiaticoside
Initial	0
1st month	7.37
2nd month	13.6
3rd month	16.41

$$\%\text{loss} = \frac{\text{initial - final\% labeled amount}}{\text{initial\% labeled amount}} \times 100$$

Adhesive property study

Table 28 displayed adhesive properties of film formulation containing *Centella asiatica* extract at 0, 1, 2 and 3 months period. The results were tested by the analysis of variance (ANOVA) at significant level 0.05. According to analytical statistics, adhesive force reduced significantly after the stress condition for 3 months. This might be resulted to the inappropriate packaging of the moisture sensitive product.

Table 28 Adhesive properties data of asiaticoside in film formulation in stability test (mean ± SD)

Periods	Force of adhesion (N/cm^2)
Initial	3.703 ± 1.11
1st month	2.927 ± 0.64*
2nd month	2.825 ± 0.11*
3rd month	2.523 ± 0.29*

* Significant at *P value* = 0.05

Mechanical properties study

Table 29 showed mechanical properties of film formulation containing *Centella asiatica* extract at 0, 1, 2 and 3 months period. The results were tested by the analysis of variance (ANOVA) at significant level 0.05. According to analytical statistics, it was found that tensile strength reduced significantly, %elongation increased significantly and work of failure and Young's modulus differ no significant. As a result, film was soft and tough after the stress condition for 3 months due to water content in film formulation increased that would be supported by the endothermic energy increased in DSC thermogram (Figure 33). The similar reason explains the result as in the adhesive property study. In the case of moisture sensitive product such as adhesive film, the appropriate packaging was most important to physical and chemical properties of the film.

Table 29 Mechanical properties data of asiaticoside in film formulation in stability test (mean ± SD)

Periods	Tensile Strength (MPa)	%Elongation	Work of Failure (mJ)	E-Mod (MPa)
Initial	15.11 ± 2.32	232.73 ± 17.50	12.24 ± 2.19	5.81 ± 1.18
1st month	6.71 ± 0.72*	364.27 ± 26.85*	12.49 ± 1.63	3.54 ± 0.45
2nd month	5.87 ± 2.61*	507.47 ± 29.50*	20.27 ± 8.31	3.76 ± 1.33
3rd month	3.69 ± 0.13*	472.63 ± 19.90*	12.03 ± 0.52	3.46 ± 0.01

* Significant at *P value* = 0.05

Differential scanning calorimetric thermograms

The application of DSC thermogram change effectively investigates the physicochemical stability of the film formulation containing *Centella asiatica* extract. As the results of the DSC thermograms of the film formulation, no change in DSC thermograms between three months of stability study as compared to that at the initial was observed. Consequently, the film formulation led to no change in physicochemical properties after the stress condition for 3 months (Figure 33). The *Centella* extract showed the stable existence in film as an amorphous state. Additionally, The very broad endothermic peaks of films formulation containing *Centella* extract after the stress condition at 0, 1, 2 and 3 months were found to be in

range 40-120°C. Moreover, the endothermic energy of peaks after the stress condition at 0, 1, 2 and 3 month were found to be 486.19 mJ, 389.49 mJ, 1120.18 mJ and 719.42 mJ, respectively. These peaks were caused by the loss of moisture absorbed or dehydration in the films (Wang et al., 2002). The endothermic energy after storage were observed clearly higher than that of initial time. These results were conformed that the film prepared tamarind seed xyloglucan had hygroscopic properties. The finding might be explainable to the decomposition by hydrolysis of asiaticoside to asiatic acid in the film, the decrease of adhesive force and the change of mechanical properties of the film.

Powder X-ray Diffractometry

The powder x-ray diffraction study was carried out to elevating film formulation containing *Centella asiatica* extract. No change in diffractograms between three months of stability study was found when compared with that at the initial time. These results were conformed the DSC study that the film formulation did not change in physicochemical properties after the stress condition for 3 months (Figure 34). The diffraction peak correspond to crystallinity of *Centella asiatica* extract in all diffractograms was not observed.

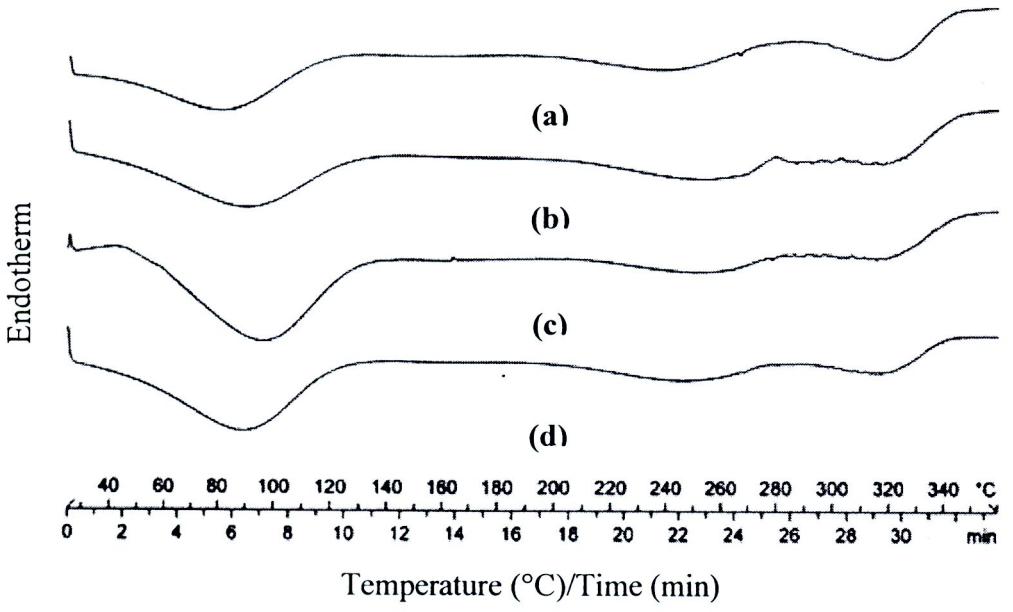

Figure 33 DSC thermograms of film formulation after stress condition (40° C, 75% RH);

(a) at initial time

(b) at first month

(c) at second month

(d) at third month

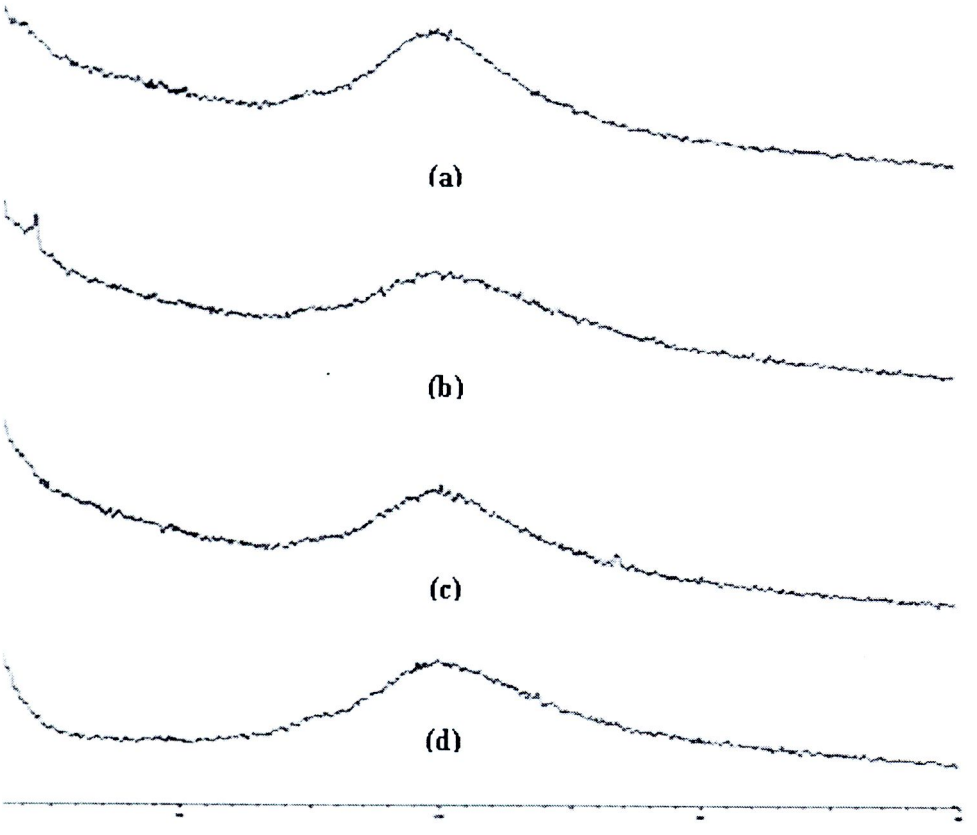

Figure 34 X-ray diffractograms of film formulation after stress condition (40° C, 75% RH);

(a) at initial time

(b) at first month

(c) at second month

(d) at third month